frontiers | Frontiers in Chemistry

TYPE Mini Review
PUBLISHED 29 August 2023
DOI 10.3389/fchem.2023.1258035

OPEN ACCESS

EDITED BY
Marco Sacchi,
University of Surrey, United Kingdom

REVIEWED BY
Tomás González-Lezana,
Spanish National Research Council (CSIC), Spain
Masashi Tsuge,
Hokkaido University, Japan

*CORRESPONDENCE
Koichiro Yamakawa,
yamakawa.koichiro@jaea.go.jp
Hirokazu Ueta,
ueta.hirokazu@jaea.go.jp

RECEIVED 13 July 2023
ACCEPTED 27 July 2023
PUBLISHED 29 August 2023

CITATION
Ueta H, Fukutani K and Yamakawa K (2023), Fast ortho-to-para conversion of molecular hydrogen in chemisorption and matrix-isolation systems.
Front. Chem. 11:1258035.
doi: 10.3389/fchem.2023.1258035

Fast ortho-to-para conversion of molecular hydrogen in chemisorption and matrix-isolation systems

Hirokazu Ueta[1]*, Katsuyuki Fukutani[1,2] and Koichiro Yamakawa[1]*

[1]Advanced Science Research Center, Japan Atomic Energy Agency, Ibaraki, Japan, [2]Institute of Industrial Science, The University of Tokyo, Tokyo, Japan

Molecular hydrogen has two nuclear-spin modifications called *ortho* and *para*. Because of the symmetry restriction with respect to permutation of the two protons, the *ortho* and *para* isomers take only odd and even values of the rotational quantum number, respectively. The *ortho*-to-*para* conversion is promoted in condensed systems, to which the excess rotational energy and spin angular momentum are transferred. We review recent studies on fast *ortho*-to-*para* conversion of hydrogen in molecular chemisorption and matrix isolation systems, discussing the conversion mechanism as well as rotational-relaxation pathways.

KEYWORDS

hydrogen, nuclear spin, rotational energy, adsorption, surface, matrix isolation

1 Introduction

Molecular hydrogen has a remarkable feature of nuclear-spin isomers. According to the quantum number I of the total nuclear spin, a hydrogen molecule has two modifications called *ortho* ($I = 1$) and *para* ($I = 0$) species. Because of the symmetry restriction, *ortho* (*para*) H_2 takes only odd (even) values of the rotational quantum number J. Whereas the transition between *ortho* and *para* species is strictly forbidden in the isolated state, it is significantly promoted upon interaction with other substances. Because the nuclear-spin isomers are identified by I and J, the *ortho*-to-*para* (*o*-*p*) conversion of H_2 involves two aspects of the nuclear-spin flip and the rotational-energy transfer to a surface or a surrounding material.

The gas-surface energy transfer has been one of the main topics in surface physics and chemistry; a typical example is the adsorption event, where the translational and adsorption energy of a molecule is transferred to a surface. In addition to the translational energy, internal degrees of freedom such as molecular vibration and rotation are also of considerable importance. Owing to the advance in laser techniques, the relaxation processes of vibrationally-excited molecules have been well studied to date (Beckerle et al., 1990; Chang and Ewing, 1990; Morin et al., 1992; Laß et al., 2005; Chen et al., 2019; Kumar et al., 2019). Compared to the vibration, on the other hand, the energy transfer from the molecular rotation to surface degrees of freedom has been poorly understood. One promising approach for the elucidation of the rotational-energy transfer is to investigate the *o*-*p* conversion of H_2 on surfaces and in matrices. After adsorption on a cold surface or trapping in a matrix, *ortho* (*para*) H_2 predominantly occupies its lowest rotational level with $J = 1$ ($J = 0$). Upon *o*-*p* conversion of H_2, the rotational-energy needs to be dissipated into surface or matrix degrees of freedom.

The *o-p* conversion of H_2 has been observed on various systems (Fukutani and Sugimoto, 2013). The *o-p* conversion is closely related to the quest for efficient ways of the H_2 storage (Ilisca, 2021), and therefore is being investigated not only on surfaces but also inside solids (Lavrov and Weber, 2002; Hiller et al., 2007; Peng et al., 2009) and nano-cages (Carravetta et al., 2004; Carravetta et al., 2006; Carravetta et al., 2007). Stimulated by the development of the experimental investigations, several conversion mechanisms have been also proposed depending on the interacting materials (Yamakawa and Fukutani, 2020): the Wigner model (Wigner, 1933), where the proton spin interacts with the inhomogeneous magnetic field generated by localized paramagnetic ions; the electron-spin-induced conversion models categorized into the second- (Ilisca, 1991) and third-order (Ilisca and Ghiglieno, 2016) perturbation theories, where the virtual electron exchange or transfer between H_2 and a surface is involved along with the Fermi contact interaction between an electron and a proton in H_2; the electric-field-induced conversion model (Sugimoto and Fukutani, 2011), where the Stark, spin-orbit, and Fermi-contact couplings mix the *ortho* and *para* states.

In spite of the extensive studies on the H_2 *o-p* conversion in the last decades, there still remain controversial issues; one is fast conversion and the other is the rotational-energy dissipation. In contrast to the *o-p* conversion time of ~10^3 s or longer observed on various surfaces and in solids, H_2 *o-p* conversion with a time constant shorter than ~10^2 s was recently observed on Pd(210) and inside a molecular solid of CO_2. On the Pd(210) surface, furthermore, rotational-energy transfer was investigated in detail taking account of electrons and phonons of surfaces. In this review paper, we expound the studies of the fast *o-p* conversion in a CO_2 matrix (Section 2) and on Pd(210) (Section 3), discussing the spin and rotational-energy transfer.

2 Matrix isolation system

The techniques of nuclear magnetic resonance (NMR), neutron scattering, Raman spectroscopy, and infrared absorption spectroscopy have been applied to *in situ* observation of the H_2 conversion in fullerene (C_{60}) (Carravetta et al., 2004; 2006; 2007), metal-organic frameworks (MOFs) (FitzGerald et al., 2010), porous coordination polymers (Kosone et al., 2015), semiconductors (Lavrov and Weber, 2002; Hiller et al., 2007; Peng et al., 2009), and viscous organic solutions (Aroulanda et al., 2007), as was reviewed recently (Ilisca, 2021). Whereas NMR directly probes the nuclear spin, the other methods enable one to resolve the rotational states of *ortho-* and *para*-H_2. In the nuclear-spin conversion study of polyatomic molecules such as H_2O (Fajardo et al., 2004; Abouaf-Marguin et al., 2007; Fillion et al., 2012), NH_3 (Boissel et al., 1993; Gauthier-Roy et al., 1993; Ruzi and Anderson, 2013), and CH_4 (Miyamoto et al., 2008; Sugimoto et al., 2015; Sugimoto and Yamakawa, 2021), the most popular technique has been rovibrational spectroscopy combined with the matrix-isolation method, where target molecules are isolated in molecular solids, e.g., rare-gas ones. Indeed, the temperature dependence of the conversion rate has been intensively studied in this way to reveal the pathways for the rotational relaxation (Sugimoto et al., 2015; Turgeon et al., 2017; Yamakawa et al., 2017).

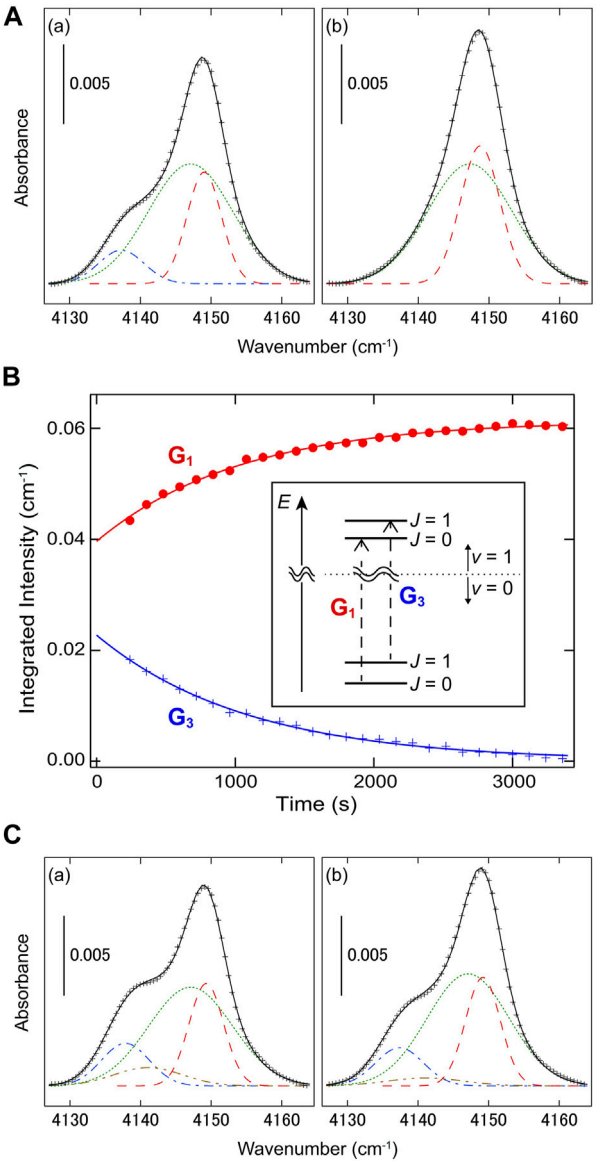

FIGURE 1
Nuclear spin conversion of H_2 trapped in solid CO_2 at 5.4 K (Yamakawa et al., 2020) (Copyright 2020; American Physical Society). **(A)** Induced infrared-absorption bands of H_2 (a) 240 s and (b) 3,360 s after the sample deposition. The result of multi-gaussian fitting is also shown; the gaussian curves of G_1, G_2, and G_3, are represented by dashed, dotted, and dashed-dotted lines, respectively. **(B)** The integrated intensities of G_1 and G_3 are plotted against time. The solid lines denote the result of monoexponential fitting. The vibrational transitions of H_2 corresponding to G_1 and G_3 are schematically shown in the inset. **(C)** Induced infrared-absorption bands of H_2 (a) 0 s and (b) 120 s after the sample deposition. The result of tetra-gaussian fitting is also shown; G_1, G_2, G_3, and G_4, are denoted by dashed, dotted, dashed-dotted, and dashed double-dotted lines, respectively.

Since H_2 is the lightest molecule and has a relatively small interaction with matrix molecules, rather low temperatures (typically T < 15 K) are required to suppress its diffusion and formation of aggregates. In previous studies, the *ortho* and *para* isomers of H_2 have been separately detected in various matrices of Ar, Kr, Xe, N_2, and CO by using Raman spectroscopy (Prochaska and Andrews, 1977; Alikhani et al., 1989; Kornath et al., 1999). In

particular, Alikhani *et al.* kept Ar-isolated H_2 at 9 K for 24 h and observed no change of the intensity ratio of the *ortho* and *para* signals, which means the *o-p* conversion was suppressed significantly in solid Ar. In contrast, comparing the ratio with a calculated value, the *o-p* conversion was found to partially proceed just during the sample deposition; they pointed out the possibility that this conversion was catalyzed by O_2 impurities. Although H_2 has no permanent electric dipole moment, one is able to detect matrix-isolated H_2 also by infrared absorption spectroscopy because of its weak polarization. Warren et al. measured infrared spectra of H_2 trapped inside Ar, Kr, N_2, and CO matrices in the wavenumber regions of pure rotational and vibrational transitions; except for the rotational spectrum of Kr-isolated H_2, the *ortho* and *para* signals were resolved (Warren et al., 1980). They also found the *ortho*-to-*para* ratio of H_2 trapped in solid Ar to be decreased by ~25% after 2–3 days and attributed this *o-p* conversion to the accidental contamination of magnetic impurities, though the accurate conversion rate was not determined. In a recent study (Yamakawa et al., 2020), H_2 was trapped and polarized in solid CO_2, so that the conversion rate of H_2 was derived from the time evolution of its infrared absorption band, as is expounded below.

The room-temperature gaseous mixture of CO_2 and H_2 at a molar ratio of $CO_2/H_2 = 100$ was condensed onto a gold substrate at 5.4 K for 10 min, and infrared spectra were measured in the reflection configuration. From the film interference pattern appearing in the baseline of the spectrum, the thickness of the CO_2 matrix was determined to be 4.5 μm. Just after the condensation, the spectrum showed not only intense absorption bands of CO_2 but also a weak band of H_2. At a trapping site of H_2, the electric fields generated by surrounding CO_2 molecules did not cancel each other out, resulting in slight electric-polarization of H_2. The time evolution of the H_2 band after the sample deposition is displayed in Figure 1A. The absorption band was well-reproduced by the combination of three gaussian curves: G_1 at 4,149 cm^{-1}, G_2 at 4,147 cm^{-1}, and G_3 at 4,138 cm^{-1}. Whereas G_1 grew with increasing time, G_3 decayed and finally disappeared. This time development was attributed to the conversion of H_2 from *ortho* to *para*; in other words, G_1 and G_3 were assigned to the Q_1 (0) and Q_1 (1) transitions of *para*- and *ortho*-H_2, respectively. In the gas phase, the transition energy of Q_1 (0), 4,161.1 cm^{-1}, is also higher than that of Q_1 (1), 4,155.3 cm^{-1} (Dabrowski, 1984), owing to the rovibrational coupling in H_2. As shown in Figure 1B, the integrated intensities of G_m (m = 1, 3) were analyzed as a function of time, and were found to follow the monoexponential function:

$$I_m(t) = [I_m(0) - I_m(\infty)] \exp(-k_m t) + I_m(\infty),$$

where $I_m(0)$ and $I_m(\infty)$ denotes the initial and equilibrium intensities, respectively. The conversion rate derived from G_1, $k_1 = (9.6 \pm 0.4) \times 10^{-4}$ s^{-1}, coincided within error with that from G_3, $k_3 = (9.2 \pm 0.4) \times 10^{-4}$ s^{-1}.

To reveal the origin of G_2, Yamakawa *et al.* also investigated the time evolution of the infrared spectrum just after the sample deposition, as shown in Figure 1C; in the time range of $t = 0 - 120$ s, an additional component, G_4, was detected at 4,141 cm^{-1}, and the decay of G_4 was observed simultaneously with the growth of G_2. Thus, it was likely that there were two kinds of trapping sites for H_2 inside solid CO_2; while G_1 and G_3 were attributed to H_2 at site A, G_2 (G_4) was to *para* (*ortho*) H_2 at site B. The frequency difference between the *para* and *ortho* species at site B was about a half of that at site A. This suggests the approach of the lowest rotational levels of *ortho*- and *para*-H_2 and relatively high anisotropy of the confining potential at site B. Note that the estimated *o-p* conversion rate at site B was as high as 6×10^{-3} s^{-1}. In a previous study with use of electron-energy-loss spectroscopy, the conversion rate of H_2 adsorbed on the stepped surface of Cu(510), where the adsorption potential is strongly anisotropic, was evaluated to be on the order of 1 s (Svensson and Andersson, 2007). These results suggest fast conversion of rotationally hindered H_2, which is also shown in Section 3.

In most of the condensed systems, the vibrational-frequency shift of H_2 with respect to the gas phase, ΔQ_1 (0), was negative: −12 (−14) cm^{-1} at site A (B) of solid CO_2 (Yamakawa et al., 2020), −17 cm^{-1} in solid N_2 and CO (Warren et al., 1980), −20 cm^{-1} on amorphous D_2O ice (Hixson et al., 1992). Despite the relatively small red-shift, the conversion rate of H_2 in solid CO_2 at 5.4 K was even higher than that on amorphous H_2O ice at 9.2 K, 2.4×10^{-4} s^{-1}, measured by Ueta et al., 2016, who also reported the monotonical increase of the rate with temperature below 14 K. This result is not explained by the electric-field-induced conversion mechanism (Sugimoto and Fukutani, 2011); instead, probable is the three-step conversion model (Ilisca and Ghiglieno, 2016; Ilisca, 2018), which consists of electron exchange between H_2 and a solvent, hyperfine contact interaction in H_2, and spin-orbit interaction inside the solvent.

Interestingly enough, the conversion time-constants (the inverse of the conversion rate) of H_2 in non-magnetic systems accompanied by energy gaps are distributed quite widely: a few or tens of minutes in MOFs (FitzGerald et al., 2010) and solid CO_2 (Yamakawa et al., 2020), and tens or hundreds of hours in crystalline Si (Lavrov and Weber, 2002; Hiller et al., 2007; Peng et al., 2009) and the cage of C_{60} (Chen et al., 2013). Note that the CO_2 film deposited below ~9 K has a porous structure with the enhanced surface area and exhibits a unique feature of "thermal spikes", which are abrupt temperature rises due to the structural rearrangement during the film deposition (Arakawa et al., 1979). The enhanced *o-p* conversion of H_2 is possibly related to the characteristically unstable and porous structure of the CO_2 film. In order to further investigate the origin of the large difference in the conversion time, the electronic structure of the H_2-solvent system, including the anisotropy of a confining potential, should be also studied. The temperature dependence of the conversion rate of H_2 trapped in matrices is under investigation and will bring about information on the channels of the rotational relaxation, just like the surface system described in the following section.

3 Molecular chemisorption system

As typical adsorption schemes of H_2, dissociative chemisorption and molecular physisorption are recognized. In most of past studies on *o-p* conversion at surfaces, H_2 in the physisorption state via the van der Waals interaction was focused, in which the molecule is in a nearly-free rotational state (Stulen, 1988; Sugimoto and Fukutani, 2014). On the other hand, some stepped surfaces exhibit a peculiar adsorption of molecular chemisorption (Mårtensson et al., 1986; Svensson et al., 1999; Schmidt et al., 2001; Sun et al., 2004; Svensson and Andersson, 2007; Christmann, 2009; Shan et al., 2009), in which the adsorption potential is anisotropic with respect to the molecular-axis angle and the rotational motion is strongly hindered. Although the rotational state is modified under the anisotropic potential, the rotational state of H_2 chemisorbed

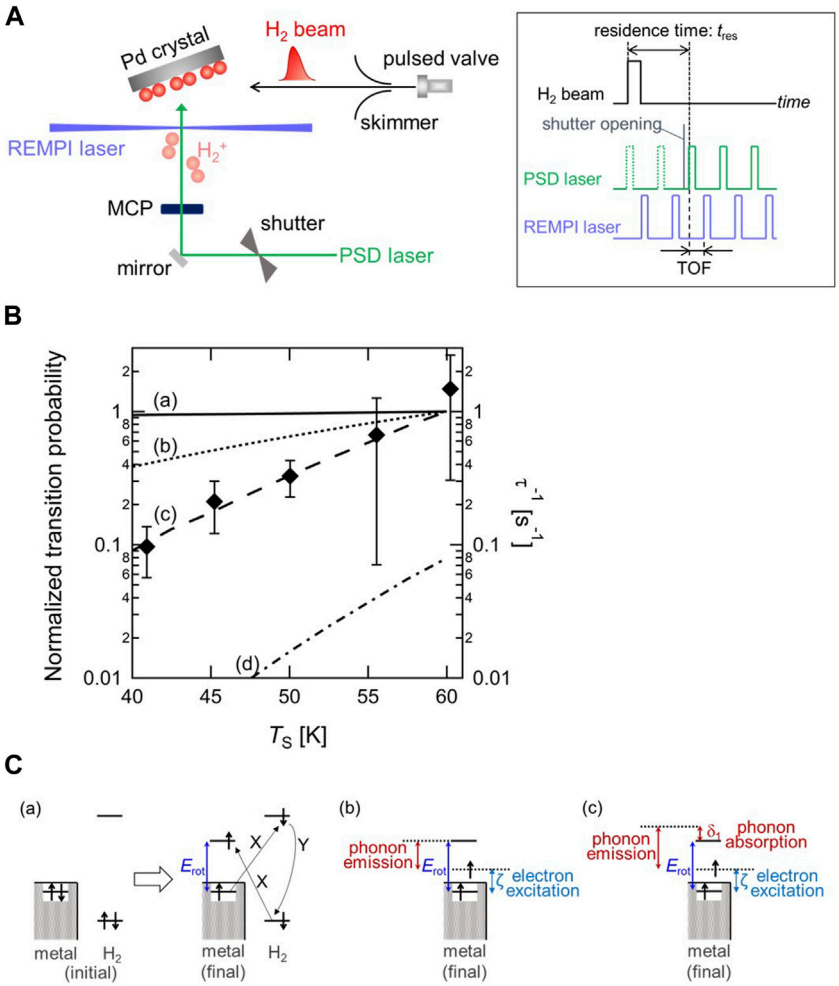

FIGURE 2
(A) Schematic diagram of the experimental setup and pulse sequence driving the molecular beam and two lasers for the *o-p* conversion measurement (Ueta et al., 2020) (Copyright 2020; American Physical Society). **(B)** Surface temperature dependence of the *o-p* conversion rate (τ^{-1}) with calculated *o-p* transition probability through (a) the *XY* model (solid line), (b) a combination model of electron transition and one-phonon process (dotted line), and (c) a combination model of electron transition and two-phonon process (dashed line). The value of transition probability at T_S = 60 K is normalized to 1 for three models. On the other hand, (d) the *p-o* transition probability through a combination model of electron transition and two-phonon process at T_S = 60 K is normalized to the value of the *o-p* transition probability through the same model at the same T_S (dashed-dotted line). Note that the experimentally determined conversion rates correspond to right axis, and the results of model calculation correspond to left axis (Ueta and Fukutani, 2023) (Copyright 2023 American Chemical Society). **(C)** Schematic illustration of the rotational-energy transfer in *o-p* conversion through (a) the *XY* model, (b) the electronic excitation and one-phonon process, and (c) the electronic excitation and two-phonon process. *X* and *Y* denotes the Coulomb interaction and the Fermi contact hyperfine interaction, respectively (Ueta and Fukutani, 2023) (Copyright 2023 American Chemical Society).

on surfaces is correlated with the nuclear-spin state, either *ortho* or *para*. In the past, while the occurrence of fast *o-p* conversion under an anisotropic potential was indicated for the systems of Cu(510) and Pd(210), direct evidence was lacking due to the limited time resolution of the experimental technique used in previous studies (Svensson and Andersson, 2007; Ohno et al., 2018). In this section, fast *o-p* conversion and associated rotational-energy transfer are discussed for H_2 molecularly chemisorbed on Pd(210).

The Pd(210) surface has (100) terraces with steps running along the [001] direction forming open (110)-like microfacets. H_2 chemisorbs on the step-edge of Pd atoms, so that H_2 binds strongly to the surface compared with the physisorption systems (Schmidt et al., 2001). The adsorption state of H_2 has been studied experimentally and theoretically (Lischka and Groß, 2002; Arguelles and Kasai, 2018a; Arguelles and Kasai, 2018b). The H_2 adsorption potential is highly anisotropic, which induces lifting of the rotational state degeneracy of the triply degenerate J = 1 state in gas-phase into doubly degenerate state (m = ±1, m: z component of J) and a non-degenerate state (m = 0) in the adsorption state. Hence the lowest *o*-H_2 (m = ±1) behaves like a two-dimensional rotor (Svensson et al., 1999).

To track the fast *o-p* conversion directly, a new experimental method was developed by combining a pulsed molecular beam (MB), photo-stimulated desorption (PSD), and resonance-enhanced multiphoton ionization (REMPI). Figure 2A shows a schematic diagram of the experimental setup and a timing chart of the MB-PSD–REMPI measurement for probing the time evolution of the rotational states of H_2 on surfaces (Ueta et al., 2020). Probing the change in the rotational state distribution allows us to track *o-p* conversion owing to the fact that the rotational states of H_2 couple with nuclear spins. With *n*-H_2 molecular beam deposition, the *o-p* ratio

at a surface temporarily becomes out-of-thermal-equilibrium, and then relaxes to the thermal equilibrium. From the change in the two nuclear-spin-state populations as a function of the adsorption time, the conversion rate can be determined, similar to that shown in Figure 1B. The conversion rate has been successfully determined on Pd(210) as a function of the surface temperature (T_S) in the range of 41–60 K as shown in Figure 2B. It is found the conversion rate increases with increasing temperature. Note that the values of the conversion time (inverse of conversion rate) are on the order of 1–10 s, demonstrating the occurrence of fast conversion on Pd(210).

Since the *o-p* conversion is accompanied by the rotational transition as well as the nuclear spin flip, the surface temperature dependence of *o-p* conversion allows us to investigate the rotational-energy (E_{rot}) transfer process in *o-p* conversion. The rotational-energy dissipation process has been discussed in previous studies on the *o-p* conversion of physisorbed H_2 on amorphous solid water, silicate and carbon materials (Ueta et al., 2016; Tsuge et al., 2021; Tsuge et al., 2021). These studies suggested that substrate phonons play an important role in the rotational-energy transfer in the conversion. Depending on the substrate, two kinds of phonon dissipation process have been considered in those studies; one-phonon and two-phonon processes. Whereas in the former process the rotational energy is dissipated into the surface by excitation of a phonon, the latter process proceeds via the simultaneous absorption of a phonon from the initial up to an intermediate state, and the emission of another from the intermediate to the final states (Scott and Jeffries, 1962). Since those materials are all non-metallic, the influence of surface electrons in the rotational-energy transfer process can be neglected.

On the other hand, Pd is a non-magnetic metal, where substrate electrons are expected to play an important role in analogy with the vibrational-energy relaxation. A widely accepted conversion model on a non-magnetic metal surface is the electron-exchange-hyperfine-contact (*XY*) model proposed by Ilisca (Ilisca, 1991) (Figure 2C-(a)). In this model, an electron in the σ_g orbital of H_2 is excited to the surface and an electron in the surface is excited to the σ_u orbital of H_2 with the Coulomb interaction, followed by nuclear-spin flip with the Fermi contact hyperfine interaction between the electron in the σ_u orbital and the hydrogen nuclei leading to the *o-p* conversion. Consequently, a surface electron is excited to the level above the Fermi level (E_F) by the amount of E_{rot}, and thus E_{rot} is dissipated into metal *electron-hole* pairs. Assuming that the electron transfer probability is independent of its energy, the *o-p* transition probability in this model is proportional to the numbers of electron and hole states available. The calculated transition probabilities are plotted in Figure 2B, showing that the transition probability does not change significantly with T_S, which is inconsistent with the experimental data. Therefore, two combination models based on the *XY* model, namely, E_{rot} transfer is shared by both electronic transition and phonon excitation through either one-phonon or two-phonon processes, are proposed (Figure 2C-(b)(c)). It should be mentioned that the electron transition process is essential for nuclear-spin flip via the Fermi contact hyperfine interaction. The results of both combination models in Figure 2B show that the transition probability varies substantially with T_S in contrast with the result based on the *XY* model. Particularly, the tendency of the combination model of electronic transition and two-phonon process is in good agreement with that of the experimentally determined *o-p* conversion rate. This indicates that the rotational energy of H_2 transfers into not only electrons but also phonons of surfaces (Ueta and Fukutani, 2023).

Recalling the fact that the vibrational energy is transferred to electrons at metal surfaces, this rotational-energy transfer process might be counterintuitive, because E_{rot} is transferred into phonons as well as electrons of surfaces despite a metallic surface. The difference between vibrational- and rotational-energy transfer paths could be ascribed to the energy scale of both degrees of freedom. While the magnitude of the rotational energy of H_2 (~10 meV) is much smaller than the vibrational energy such as the CO stretch mode (~0.26 eV), that is comparable with the magnitude of the substrate phonon energy. The energy transfer path might be determined by the energy-scale matching between the molecular degree of freedom and surfaces as a receiver.

4 Concluding remarks

We have expounded a recent advance in the *o-p* conversion study of H_2, dealing with the fast conversion in the two novel systems characterized by the matrix isolation and molecular chemisorption. It is notable that the conversion time-scale was ~10^2 s or shorter in spite of the non-magnetic properties of these systems. While a variety of metal oxides have been investigated as the magnetic catalysts of the H_2 *o-p* conversion for many decades, expanding needs for the efficient H_2 storage and high-performance electrodes for the water electrolysis promotes the studies of H_2 interacting with non-magnetic substances such as MOFs and carbon nanomaterials. Since the *o-p* conversion involving both the spin- and energy-transfers influences the storage and chemical reaction of H_2, further studies of the conversion mechanism in the non-magnetic systems are required to reveal the determinant of the conversion time-scale. The anisotropy of a confining potential should be one of the key factors, and the temperature dependence of the conversion rate will provide essential information on the rotational-relaxation pathways also in other systems.

Author contributions

HU: Writing–original draft, Writing–review and editing. KF: Writing–review and editing. KY: Writing–original draft, Writing–review and editing.

Funding

The authors declare financial support was received for the research, authorship, and/or publication of this article. This work was supported by the Japan Society for the Promotion of Science (KAKENHI; Grant JP18H05518, JP20K05424, JP20K05337, JP21H04650, JP23H01856, and JP23K04593) and Grant for Basic Science Research Projects from the Sumitomo Foundation. HU was partially supported by MEXT Japan, Leading Initiative for Excellent Young Researchers.

Conflict of interest

The authors declare that the research was conducted in the absence of any commercial or financial relationships that could be construed as a potential conflict of interest.

Publisher's note

References

Abouaf-Marguin, L., Vasserot, A. M., Pardanaud, C., and Michaut, X. (2007). Nuclear spin conversion of water diluted in solid argon at 4.2K: Environment and atmospheric impurities effects. *Chem. Phys. Lett.* 447 (4–6), 232–235. doi:10.1016/j.cplett.2007.09.014

Alikhani, M. E., Silvi, B., Perchard, J. P., and Chandrasekharan, V. (1989). Reinvestigation of the Raman spectra of dihydrogen trapped in rare gas solids. I. H_2, HD, and D_2 monomeric species. *J. Chem. Phys.* 90 (10), 5221–5231. doi:10.1063/1.456475

Arakawa, I., Kobayashi, M., and Tuzi, Y. (1979). Effects of thermal spikes on the characteristics of cryosorption pumps with condensed carbon dioxide layers. *J. Vac. Sci. Technol.* 16 (2), 738–740. doi:10.1116/1.570072

Arguelles, E. F., and Kasai, H. (2018a). Bound nuclear spin states of H_2 in an anisotropic potential induced by a stepped metal surface. *J. Vac. Sci. Technol. A Vac. Surfaces, Films* 36 (3), 030601. doi:10.1116/1.5023158

Arguelles, E. F., and Kasai, H. (2018b). Hindered rotation and nuclear spin isomers separation of molecularly chemisorbed H_2 on Pd(210). *J. Appl. Phys.* 123 (11), 115301. doi:10.1063/1.5021994

Aroulanda, C., Starovoytova, L., and Canet, D. (2007). Longitudinal nuclear spin relaxation of ortho- and para-hydrogen dissolved in organic solvents. *J. Phys. Chem. A* 111 (42), 10615–10624. doi:10.1021/jp073162r

Beckerle, J. D., Casassa, M. P., Cavanagh, R. R., Heilweil, E. J., and Stephenson, J. C. (1990). Ultrafast infrared response of adsorbates on metal surfaces: Vibrational lifetime of CO/Pt(111). *Phys. Rev. Lett.* 64 (17), 2090–2093. doi:10.1103/PhysRevLett.64.2090

Boissel, P., Gauthier-Roy, B., and Abouaf-Marguin, L. (1993). Dipolar interactions between NH_3 molecules trapped in solid argon. II. Line narrowing during nuclear spin species conversion. *J. Chem. Phys.* 98 (9), 6835–6842. doi:10.1063/1.464775

Carravetta, M., Danquigny, A., Mamone, S., Cuda, F., Johannessen, O. G., Heinmaa, I., et al. (2007). Solid-state NMR of endohedral hydrogen–fullerene complexes. *Phys. Chem. Chem. Phys.* 9 (35), 4879–4894. doi:10.1039/B707075F

Carravetta, M., Johannessen, O. G., Levitt, M. H., Heinmaa, I., Stern, R., Samoson, A., et al. (2006). Cryogenic NMR spectroscopy of endohedral hydrogen-fullerene complexes. *J. Chem. Phys.* 124 (10), 104507. doi:10.1063/1.2174012

Carravetta, M., Murata, Y., Murata, M., Heinmaa, I., Stern, R., Tontcheva, A., et al. (2004). Solid-state NMR spectroscopy of molecular hydrogen trapped inside an open-cage fullerene. *J. Am. Chem. Soc.* 126 (13), 4092–4093. doi:10.1021/ja031536y

Chang, H.-C., and Ewing, G. E. (1990). Infrared fluorescence from a monolayer of CO on NaCl(100). *Phys. Rev. Lett.* 65 (17), 2125–2128. doi:10.1103/PhysRevLett.65.2125

Chen, J. Y.-C., Li, Y., Frunzi, M., Lei, X., Murata, Y., Lawler, R. G., et al. (2013). 'Nuclear spin isomers of guest molecules in $H_2@C_{60}$, $H_2O@C_{60}$ and other endofullerenes', *Philosophical Trans. R. Soc. A Math. Phys. Eng. Sci.*, 371, p. 20110628. doi:10.1098/rsta.2011.0628

Chen, L., Lau, J. A., Schwarzer, D., Meyer, J., Verma, V. B., and Wodtke, A. M. (2019). The Sommerfeld ground-wave limit for a molecule adsorbed at a surface. *Science* 363 (6423), 158–161. doi:10.1126/science.aav4278

Christmann, K. (2009). Interaction of hydrogen with (210)-oriented metal surfaces: Molecular precursors, chemisorbed atoms and subsurface states. *Surf. Sci.* 603 (10–12), 1405–1414. doi:10.1016/J.SUSC.2008.09.066

Dabrowski, I. (1984). The lyman and werner bands of H_2. *Can. J. Phys.* 62 (12), 1639–1664. doi:10.1139/p84-210

Fajardo, M. E., Tam, S., and DeRose, M. E. (2004) 'Matrix isolation spectroscopy of H_2O, D_2O, and HDO in solid parahydrogen', *J. Mol. Struct.*, 695–696, pp. 111–127. doi:10.1016/j.molstruc.2003.11.043

Fillion, J.-H., et al. (2012). Understanding the relationship between gas and ice: Experimental investigations on ortho-para ratios. *EAS Publ. Ser.* 58, 307–314. doi:10.1051/eas/1258051

FitzGerald, S. A., Hopkins, J., Burkholder, B., Friedman, M., and Rowsell, J. L. C. (2010). Quantum dynamics of adsorbed normal- and para-H_2, HD, and D_2 in the microporous framework MOF-74 analyzed using infrared spectroscopy. *Phys. Rev. B* 81 (10), 104305. doi:10.1103/PhysRevB.81.104305

Fukutani, K., and Sugimoto, T. (2013). Physisorption and ortho–para conversion of molecular hydrogen on solid surfaces. *Prog. Surf. Sci.* 88 (4), 279–348. doi:10.1016/j.progsurf.2013.09.001

Gauthier-Roy, B., Abouaf-Marguin, L., and Boissel, P. (1993). Dipolar interactions between NH_3 molecules trapped in solid argon. I. Kinetics of the nuclear spin species conversion. *J. Chem. Phys.* 98 (9), 6827–6834. doi:10.1063/1.464774

Hiller, M., Lavrov, E. V., and Weber, J. (2007). Ortho-para conversion of interstitial H_2 in Si. *Phys. Rev. Lett.* 98 (5), 055504. doi:10.1103/PhysRevLett.98.055504

Hixson, H. G., Wojcik, M. J., Devlin, M. S., Devlin, J. P., and Buch, V. (1992). Experimental and simulated vibrational spectra of H_2 absorbed in amorphous ice: Surface structures, energetics, and relaxations. *J. Chem. Phys.* 97 (2), 753–767. doi:10.1063/1.463240

Ilisca, E. (1991). Ortho-para H_2 conversion on a cold Ag(111) metal surface. *Phys. Rev. Lett.* 66 (5), 667–670. doi:10.1103/PhysRevLett.66.667

Ilisca, E., and Ghiglieno, F. (2016). Nuclear conversion theory: Molecular hydrogen in non-magnetic insulators. *R. Soc. Open Sci.* 3 (9), 160042. doi:10.1098/rsos.160042

Ilisca, E. (2018) 'Electromagnetic nuclear spin conversion: Hydrogen on amorphous solid water', *Chem. Phys. Lett.*, 713, pp. 289–292. doi:10.1016/j.cplett.2018.10.053

Ilisca, E. (2021). Hydrogen conversion in nanocages. *Hydrogen* 2 (2), 160–206. doi:10.3390/hydrogen2020010

Kornath, A., Zoermer, A., and Köper, I. (1999) 'Raman spectroscopic studies on matrix-isolated hydrogen and deuterium. 3. Molecular dynamics in matrices', *Spectrochimica Acta Part A Mol. Biomol. Spectrosc.*, 55(13), pp. 2593–2599. doi:10.1016/S1386-1425(99)00054-2

Kosone, T., Hori, A., Nishibori, E., Kubota, Y., Mishima, A., Ohba, M., et al. (2015). Coordination nano-space as stage of hydrogen ortho–para conversion. *R. Soc. Open Sci.* 2 (7), 150006. doi:10.1098/rsos.150006

Kumar, S., Jiang, H., Schwarzer, M., Kandratsenka, A., Schwarzer, D., and Wodtke, A. (2019). Vibrational relaxation lifetime of a physisorbed molecule at a metal surface. *Phys. Rev. Lett.* 123 (15), 156101. doi:10.1103/PhysRevLett.123.156101

Lavrov, E. V., and Weber, J. (2002). Ortho and para interstitial H_2 in silicon. *Phys. Rev. Lett.* 89 (21), 215501. doi:10.1103/PhysRevLett.89.215501

Laß, K., Han, X., and Hasselbrink, E. (2005). The surprisingly short vibrational lifetime of the internal stretch of CO adsorbed on Si(100). *J. Chem. Phys.* 123 (5), 051102. doi:10.1063/1.1993550

Lischka, M., and Groß, A. (2002). Hydrogen adsorption on an open metal surface: H_2/Pd(210). *Phys. Rev. B* 65 (7), 75420. doi:10.1103/PhysRevB.65.075420

Mårtensson, A.-S., Nyberg, C., and Andersson, S. (1986). Observation of molecular H_2 chemisorption on a nickel surface. *Phys. Rev. Lett.* 57 (16), 2045–2048. doi:10.1103/PhysRevLett.57.2045

Miyamoto, Y., Fushitani, M., Ando, D., and Momose, T. (2008) 'Nuclear spin conversion of methane in solid parahydrogen', *J. Chem. Phys.*, 128(11), p. 114502. doi:10.1063/1.2889002

Morin, M., Levinos, N. J., and Harris, A. L. (1992). Vibrational energy transfer of CO/Cu(100): Nonadiabatic vibration/electron coupling. *J. Chem. Phys.* 96 (5), 3950–3956. doi:10.1063/1.461897

Ohno, S., Ivanov, D., Ogura, S., Wilde, M., Arguelles, E. F., Diño, W. A., et al. (2018). Rotational state modification and fast ortho-para conversion of H_2 trapped within the highly anisotropic potential of Pd(210). *Phys. Rev. B* 97 (8), 085436. doi:10.1103/PhysRevB.97.085436

Peng, C., Stavola, M., Fowler, W. B., and Lockwood, M. (2009). Ortho-para transition of interstitial H_2 and D_2 in Si. *Phys. Rev. B* 80 (12), 125207. doi:10.1103/PhysRevB.80.125207

Prochaska, F. T., and Andrews, L. (1977). Vibration–rotational and pure rotational laser–Raman spectra of H_2, D_2, and HD in matrices at 12 K. *J. Chem. Phys.* 67 (3), 1139–1143. doi:10.1063/1.434965

Ruzi, M., and Anderson, T. D. (2013). Matrix isolation spectroscopy and nuclear spin conversion of NH_3 and ND_3 in solid parahydrogen. *J. Phys. Chem. A* 117 (39), 9712–9724. doi:10.1021/jp3123727

Schmidt, P. K., Christmann, K., Kresse, G., Hafner, J., Lischka, M., and Groß, A. (2001). Coexistence of atomic and molecular chemisorption states: H_2/Pd(210). *Phys. Rev. Lett.* 87 (9), 096103. doi:10.1103/PhysRevLett.87.096103

Scott, P. L., and Jeffries, C. D. (1962). Spin-lattice relaxation in some rare-earth salts at helium temperatures; observation of the phonon bottleneck. *Phys. Rev.* 127 (1), 32–51. doi:10.1103/PhysRev.127.32

Shan, J., Kleyn, A. W., and Juurlink, L. B. F. (2009). Adsorption of molecular hydrogen on an ultrathin layer of Ni(111) hydride. *Chem. Phys. Lett.* 474 (1–3), 107–111. doi:10.1016/J.CPLETT.2009.04.051

Stulen, R. H. (1988). Summary Abstract: Observation of molecular H_2 and D_2 on Pd and Ag using thermal desorption between 5 and 20 K. *J. Vac. Sci. Technol. A* 6 (3), 776–778. doi:10.1116/1.575111

Sugimoto, T., and Fukutani, K. (2014). Effects of rotational-symmetry breaking on physisorption of ortho- and para-H_2 on Ag(111). *Phys. Rev. Lett.* 112 (14), 146101. doi:10.1103/PhysRevLett.112.146101

Sugimoto, T., and Fukutani, K. (2011). Electric-field-induced nuclear-spin flips mediated by enhanced spin-orbit coupling. *Nat. Phys.* 7 (4), 307–310. doi:10.1038/nphys1883

Sugimoto, T., Yamakawa, K., and Arakawa, I. (2015). Infrared spectroscopic investigation of nuclear spin conversion in solid CH_4. *J. Chem. Phys.* 143 (22), 224305. doi:10.1063/1.4936655

Sugimoto, T., and Yamakawa, K. (2021). Nuclear-spin conversion analysis of $\nu_2 + \nu_4$ combination band of crystalline methane in phase II. *J. Chem. Phys.* 154 (2), 026101. doi:10.1063/5.0031272

Sun, Q., Reuter, K., and Scheffler, M. (2004). Hydrogen adsorption on RuO_2(110): Density-functional calculations. *Phys. Rev. B* 70 (23), 235402. doi:10.1103/PhysRevB.70.235402

Svensson, K., and Andersson, S. (2007). Fast ortho-para conversion of H_2 adsorbed at copper surface step atoms. *Phys. Rev. Lett.* 98 (9), 096105. doi:10.1103/PhysRevLett.98.096105

Svensson, K., Bengtsson, L., Bellman, J., Hassel, M., Persson, M., and Andersson, S. (1999). Two-dimensional quantum rotation of adsorbed H_2. *Phys. Rev. Lett.* 83 (1), 124–127. doi:10.1103/PhysRevLett.83.124

Tsuge, M., Kouchi, A., and Watanabe, N. (2021). Measurements of ortho-to-para nuclear spin conversion of H_2 on low-temperature carbonaceous grain analogs: Diamond-like carbon and graphite. *Astrophysical J.* 923 (1), 71. doi:10.3847/1538-4357/ac2a33

Tsuge, M., Namiyoshi, T., Furuya, K., Yamazaki, T., Kouchi, A., and Watanabe, N. (2021). Rapid ortho-to-para nuclear spin conversion of H_2 on a silicate dust surface. *Astrophysical J.* 908 (2), 234. doi:10.3847/1538-4357/abd9c0

Turgeon, P.-A., Vermette, J., Alexandrowicz, G., Peperstraete, Y., Philippe, L., Bertin, M., et al. (2017). Confinement effects on the nuclear spin isomer conversion of H_2O. *J. Phys. Chem. A* 121 (8), 1571–1576. doi:10.1021/acs.jpca.7b00893

Ueta, H., and Fukutani, K. (2023). Rotational-energy transfer in H_2 ortho-paraconversion on a metal surface: Interplay between electron and phonon systems. *J. Phys. Chem. Lett.* 14, 7591–7596. doi:10.1021/acs.jpclett.3c01209

Ueta, H., Sasakawa, Y., Ivanov, D., Ohno, S., Ogura, S., and Fukutani, K. (2020). Direct measurement of fast ortho-para conversion of molecularly chemisorbed H_2 on Pd(210). *Phys. Rev. B* 102 (12), 121407. doi:10.1103/PhysRevB.102.121407

Ueta, H., Watanabe, N., Hama, T., and Kouchi, A. (2016). Surface temperature dependence of hydrogen ortho-para conversion on amorphous solid water. *Phys. Rev. Lett.* 116 (25), 253201. doi:10.1103/PhysRevLett.116.253201

Warren, J. A., Smith, G. R., and Guillory, W. A. (1980). The infrared spectrum of matrix isolated hydrogen and deuterium. *J. Chem. Phys.* 72 (9), 4901–4908. doi:10.1063/1.439774

Wigner, E. P. (1933). Uber die paramagnetische U mwandlung on Para-Orthowasserstoff. III. *Z. Phys. Chem. B* 23, 28.

Yamakawa, K., Azami, S., and Arakawa, I. (2017). Phonon-mediated nuclear spin relaxation in H_2O. *Eur. Phys. J. D* 71 (3), 70. doi:10.1140/epjd/e2017-70642-8

Yamakawa, K., and Fukutani, K. (2020). Nuclear spin conversion of H_2, H_2O, and CH_4 interacting with diamagnetic insulators. *J. Phys. Soc. Jpn.* 89 (5), 051016. doi:10.7566/JPSJ.89.051016

Yamakawa, K., Ishibashi, A., Namiyoshi, T., Azuma, Y., and Arakawa, I. (2020). Fast nuclear-spin conversion of H_2 trapped and polarized in a CO_2 matrix. *Phys. Rev. B* 102 (4), 041401. doi:10.1103/PhysRevB.102.041401